Available online at www.sciencedirect.com
ScienceDirect
Journal of Hazardous Materials 147 (2007) 633–643
Journal of Hazardous Materials
www.elsevier.com/locate/jhazmat

Adsorption of fluoride in aqueous solutions using $KMnO_4$-modified activated carbon derived from steam pyrolysis of rice straw

A.A.M. Daifullah, S.M. Yakout *, S.A. Elreefy

Hot Lab. Centre, Atomic Energy Authority, Cairo, Egypt

Received 3 August 2006; received in revised form 13 January 2007; accepted 15 January 2007
Available online 20 January 2007

Abstract

Fluoride in drinking water above permissible levels is responsible for human and skeletal fluorosis. In this study, activated carbons (AC) prepared by one-step steam pyrolysis of rice straw at 550, 650, 750 °C, respectively, were modified by liquid-phase oxidation using HNO_3, H_2O_2 and $KMnO_4$. Characterization of these 12 carbons was made by their surface area, porosity, acidity, basicity, pH_{pzc}, pH and ability to remove fluoride anion. Based on the data of the latter factor, the $RS_2/KMnO_4$ carbon was selected. Along with batch adsorption studies, which involve effect of pH, adsorbate concentration, adsorbent dosage, contact time, temperature, and Co-ions (SO_4^{2-}, Cl^-, Br^-). The effects of natural organic matter (NOM) were also made to remove the fluoride from natural water. On the basis of kinetic studies, specific rate constants involved in the adsorption process using $RS_2/KMnO_4$ carbon was calculated and second-order adsorption kinetics was observed. Equation isotherms such as Langmuir (L), Freundlich (F), Langmuir–Freundlich (LF) and Dubinin–Radushkevich (DR) were successfully used to model the experimental data. From the DR isotherm parameters, it was considered that the uptake of F^- by $RS_2/KMnO_4$ carbon proceeds by an ion-exchange mechanism ($E = 10.46\,kJ\,mol^{-1}$). The thermodynamic parameters of fluoride sorption were calculated and the sorption process was chemical in nature. The ability of $RS_2/KMnO_4$ to remove F^- from Egyptian crude phosphoric acid ($P_2O_5 = 48.42\%$) was tested and the adsorption capacity of F^- in H_3PO_4 was greater than that in distilled water. This is may be due to fluoride adsorption enhanced at lower pH of crude acid.

Keywords: Fluoride adsorption; Activated carbon; Steam activation; Surface modification

1. Introduction

Of all chemical elements in the Periodic Table, fluorine is the most electronegative and the most reactive element [1]. Because of its great reactivity, fluorine cannot be found in nature in its elemental state. It exists as fluorides.

Fluoride pollution in the environment occurs through two different channels, which are natural and anthropogenic sources. Fluoride is frequently encountered in minerals and in geochemical deposits and is generally released into subsoil water sources by the slow natural degradation of fluorine contained in rocks. Fluorine and its compounds are extensively used in industry; elemental fluorine is necessary in the preparation of many fluoride compounds, which play an important role in semiconductors, fertilizers (e.g. phosphate fertilizers), production of high purity graphite, electrolysis of alumina and in nuclear applications. Toxic wastes containing fluorine/fluoride are generated in all industries using fluorine or its compounds as a raw material [2].

The other perspective is that fluoride is recognized as essential in the human diet. Maintaining fluoride concentrations of 1 mg/l in the dietary intake can prevent particularly skeletal and dental problems. However, when the fluoride concentration is above this level, it affects the metabolism of elements such as Ca, P in human body and leads to bone diseases (fluorosis), mottling of teeth and lesions of the endocrine glands, thyroid, liver and other organs [3]. According to the World Health Organisation, the maximum acceptable concentration of fluorides is 1.5 mg/l [4]. It had been reported that the concentration of fluoride ions in groundwater of many places exceeds the permissible values [3]. So, it is imperative and significant for removing excessive fluorides from water.

There are different materials have been used for defluoridation including activated carbon (AC), tricalcium phosphate, synthetic ion exchangers, lime activated alumina, and alum. However, in recent years, considerable attention of scientists has been devoted to the study of different types of low-cost

* Corresponding author. Fax: +20 2 462 0608.
E-mail address: yakout_2004@yahoo.com (S.M. Yakout).

0304-3894/$ – see front matter © 2007 Elsevier B.V. All rights reserved.
doi:10.1016/j.jhazmat.2007.01.062

materials such as: spent bleaching earth, wollastonite and chine clay, bentonite and activated bentonite, kaolinitic clay, agricultural by products, fly ash, carbon slurry, biogas residual slurry, zeolite, bone char and flax shive [5].

Many methods have been developed to remove excessive fluoride from water, namely adsorption, ion exchange, precipitation, electrolysis, donnan dialysis, and electrodialysis [3]. Among these methods, adsorption is still one of the most extensively used methods for defluoridation of water.

Activated carbon has been proven to be an effective adsorbent for the removal of a wide variety of organic and inorganic pollutants dissolved in aqueous media. AC modification are gaining prominence due to the need to enable ACs to develop affinity for certain contaminants to cater for their removal from varying types of wastewater in the industries. It is an established fact that the AC surface can display acidic, basic and/or neutral characteristics depending on the presence of surface functional groups. As such, modification of chemical characteristics in this paper is taken to mean treatment to modify the inherent surface functional groups of AC. It has been widely recognized that chemical species removal by AC adsorption is due predominantly to the surface complex formation between the species and the surface functional groups. This is especially significant in the case of removing inorganics and metals from aqueous solutions.

The objective of the present work is to asses the ability of modified activated carbon derived from steam pyrolysis of rice straw for the removal of fluoride from water at different concentrations, contact times, temperatures, and pH, as these parameters are some of the main factors influencing the uptake of solute at the solid–solution interface.

2. Materials and methods

All solutions were prepared using sodium fluoride in double distilled water and all reagents were of A.R. grade.

2.1. Preparation of activated carbons

0.5 kg of rice straw was dried and fed into fluidized bed reactor, described elsewhere [6] at heating rate of 50 °C/10 min in presence of N_2 flow (300 ml/min). The steam was introduced with flow rate of 5 ml/min when the furnace reached 350 °C. The heating continues up to final temperature of 550, 650 and 750 °C, respectively. The hold time was 1 h. Then, furnace is switched off. The carbons were left to cool down and the products are taken the abbreviations RS_1, RS_2 and RS_3, respectively.

2.2. Liquid-phase oxidation of carbons

Activated carbons (RS_1, RS_2, RS_3) were oxidized using HNO_3, H_2O_2 and $KMnO_4$ to produce modified carbons according to the procedures described earlier [7] (cf. Table 1).

2.3. Characterization of the carbons

The surface area and pore characteristics of the prepared carbons were determined by nitrogen adsorption at 77 K using (Quantachrome Instruments, Model Nova1000e series, USA). The samples were outgased at 250 °C under N_2 flow for 16 h. The pH of a particular adsorbent is measured with pH meter (Acton, MA) as mentioned elsewhere [8]. The simple mass titration method was used to estimate the pH_{pzc} of carbons as reported [9]. The Boehm titration method [10] was used to estimate the acidic and basic properties of carbons.

2.4. Carbon selection

Fifty millilitre aliquots of F^- of initial concentration $C_o = 50$ ppm were mixed with 0.1 g of each carbon and shaken for 24 h. The filtrate was analyzed for residual F^- anion concentration using ion chromatography (IC).

2.5. Adsorption experiments

Series of experiments were carried out using 20 ml solution of F^- of initial concentration of 20 ppm using $RS_2/KMnO_4$ carbon to define the factors influencing the sorption process. In this concern, the following conditions were tested: the carbon dosages (5–100 mg), pH (2–11), temperature (25–55 °C); contact time (1–24 h). The pH of the solutions were adjusted

Table 1
Characterization of activated carbons

Notation	S_{BET} (m^2/g)	V_p (cm^3/g)	Basicity (meq/g)	Acidity (meq/g)	F^- removal, R (%)	pH_{pzc}	pH	Ash content (%)
RS_1/550	71.35	0.055	6.22	5.6	5.6	9.5	9.2	49.0
RS_2/650	76.2	0.063	8.13	2.0	5.6	9.3	9.3	44.0
RS_3/750	63.0	0.052	3.06	1.79	5.56	9.4	9.07	41.0
RS_1/HNO_3	87.2	0.118	2.79	8.93	46.56	3.0	3.23	64.1
RS_2/HNO_3	68.8	0.083	5.91	7.35	50	3.3	3.26	64.1
RS_3/HNO_3	66.3	0.081	3.14	9.26	100	2.95	3.42	66.8
RS_1/H_2O_2	110.9	0.078	5.21	3.75	5.6	8.0	8.08	59.1
RS_2/H_2O_2	96.8	0.06	3.01	2.6	5.5	7.6	7.04	57.2
RS_3/H_2O_2	85.1	0.053	6.12	5.21	10.99	5.6	6.0	52.0
$RS_1/KMnO_4$	87.75	0.095	5.29	4.39	100	8.6	8.25	57.9
$RS_2/KMNO_4$	122.9	0.1	5.77	5	100	7.8	7.8	55.8
$RS_3/KMNO_4$	91.5	0.092	6.44	4.81	100	7.8	7.7	51.2

to different values by dilute NaOH or HCl solutions after the addition of carbon to the solution.

2.6. Equilibrium isotherm

Equilibrium adsorption isotherm was determined by shaking 20 ml of F^- of initial concentration 20 mg/l with various amounts of $RS_2/KMnO_4$ carbon. The mixtures were agitated for equilibrium at different temperatures 25, 45, and 55 °C, respectively. The residual concentration was analyzed. As well as, the equilibrium isotherm was studied by using Ismailia canal surface water instead of bidistilled water to investigate the effect of natural organic matter (NOM) on F^- removal. The application of F^- removal from crude H_3PO_4 was carried out by mixing 10 ml of crude phosphoric acid with various masses (0.1–1.0 g) of $RS_2/KMnO_4$ carbon at 25 °C.

2.7. Analysis

The F^- anion concentration was determined using Metrohm 690 ion chromatography with conductivity detector. The conditions were: column: 6.1009.000 anion column super-sep; eluent: 0.5 mmol/l phathalic acid, 5% acetonitrile, pH 4.2; flow rate: 1.5 ml/min; injection volume: 100 μl; full scale: 4 μS cm; integrator: C-R5A chromatopac.

3. Results and discussion

Because rice straw is not a dense material, the activation process is facilitated and occurs much faster than with other more common carbon precursors. This outcome is desirable because short activation times result in reduced manufacturing costs. Conversely, being a soft material limits the development of very large surface areas. Surface areas for the experimental carbons were lower than for the commercial carbons. So we conduct a surface modification for these carbons to obtain the highest adsorption capacity from it as surface area alone not affect significantly on the adsorption process. Generally, it is clear that all methods agree in the order of values giving that the increase of temperature affects little on the surface area of products (RS_1, RS_2, RS_3) while upon treatment the total surface area is highly increased by treatment with KOH followed by H_2O_2 and $KMNO_4$ while HNO_3 decrease the surface area (Table 1).

It is clear that, treatment of activated rice straw with oxidizing agents leads to increasing of ash contents due to increasing the inorganic constituent such as manganese compounds (MnO_2) in case of $KMnO_4$ treatment.

Also, it is seen that the values of pH and pH_{pzc} of each sample are very close. This confirms the conclusion that the former can be taken as a good measure of the latter. This indicates that there is no leaching of inorganic oxides constituents from carbon affecting on the pH measurements of samples, so our carbons are suitable in water treatment. The carbon pH is mainly affected by functional groups on the surface, which not contribute in %ash. The results of number of basic and acidic groups of our carbons are collected in Table 1. The results indicate that acidic and basic surface sites coexist in all unoxidized and oxidized carbons. This means that these materials have amphoteric behaviour, and in general terms the more acidic samples are the less basic ones.

A preliminary screening study was conducted to assess the usefulness and abilities of our carbon materials for removal of fluorides from water (Table 1). It is clear that the fluoride sorption is dependent on large number of variables such as surface chemistry, surface charge, pore structure and concentration of functional groups, etc. and no single property appears to be dominant in anion adsorption from aqueous solutions. $RS/KMnO_4$ exhibited the highest capacity for removal of fluoride anions compared to the other carbon adsorbents. $RS_2/KMnO_4$ carbon has the highest surface area and pore volume, therefore, $RS_2/KMnO_4$ was selected for further detailed experimental investigations. The aim was to find out the effect of various parameters on its affinity towards the uptake of fluoride anions using $RS_2/KMnO_4$ carbon.

3.1. Kinetic studies of anions adsorption

3.1.1. Effect of agitation time

The time-profile of adsorption of F^- onto $RS_2/KMnO_4$ is presented in Fig. 1. As agitation time increases, anion removal also increases initially, but then gradually approaches a more or less constant value, denoting attainment of equilibrium. Obviously, the equilibrium was attained after shaking for about 3 h, beyond which there is no further increase in the adsorption. Similar equilibrium time was reported for the adsorption of fluoride onto carbon nanotube [11].

3.1.2. Kinetic rate parameters

The kinetic experimental data of fluoride ions on $RS_2/KMnO_4$ sorbent is simulated by the pseudo first-order and pseudo second-order rate equation [12].

$$\log(q_e - q) = \log q_e - \left(\frac{k_{ad}}{2.303}\right) t \qquad \text{1st order} \tag{1}$$

$$\frac{t}{q_t} = \frac{1}{k_2 q_e^2} + \frac{t}{q_e} \qquad \text{2nd order} \tag{2}$$

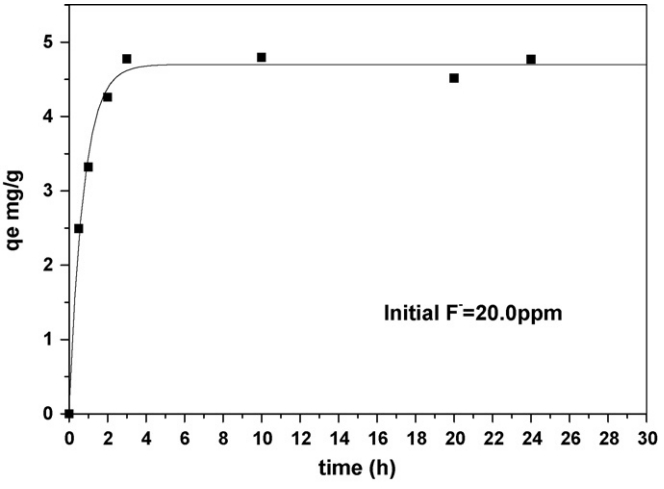

Fig. 1. Influence of agitation time on adsorption of F^- by $RS_2/KMnO_4$.

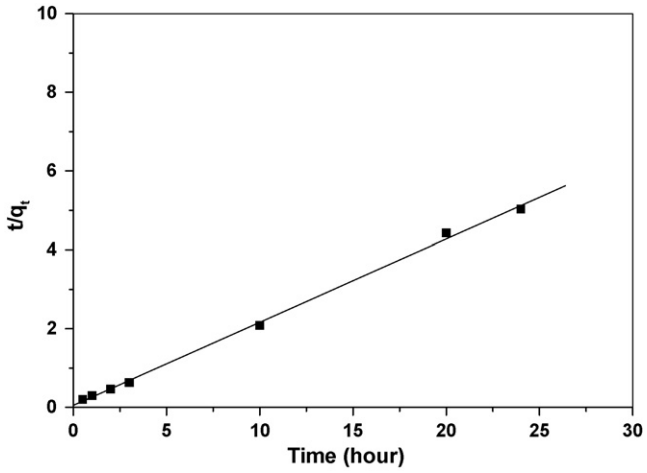

Fig. 2. Pseudo-second-order sorption kinetics of fluoride adsorption onto $RS_2/KMnO_4$.

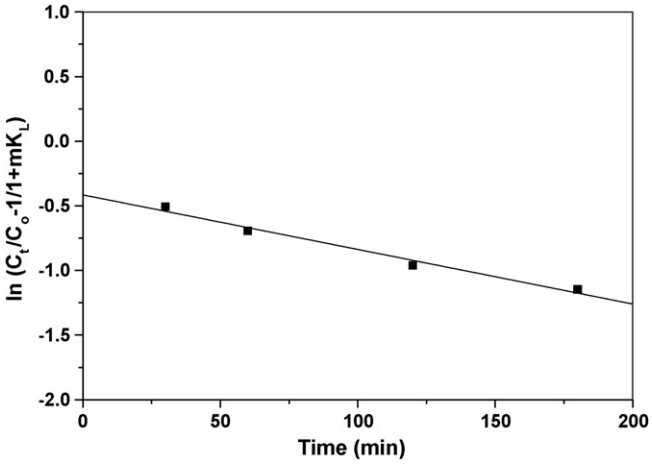

Fig. 3. Mass transfer plot for the adsorption of fluoride onto $RS_2/KMnO_4$.

where q_t and q_e are the amount of adsorbed fluoride (mg/g) at time t and at equilibrium time, respectively, and K_2 is second-rate constant of adsorption.

The results are shown in Fig. 2. The correlation coefficient R^2 for the pseudo second-order adsorption model has high value (0.998). The calculated equilibrium adsorption capacities $q_{e,cal}$ (4.7 mg/g) is consistent with the experimental (4.8 mg/g). These results suggest that the sorption system is the second order, based on the assumption that the rate-limiting step may be chemical sorption involving valency forces through sharing or exchange of electrons between anions and adsorbent [13]. Similar results were obtained by Ruixia et al. for the adsorption of fluoride onto ion-exchange fiber [14] and by Fan et al. on low-cost materials [15].

3.1.3. Surface mass transfer coefficient

Mass transfer analysis for the removal of fluoride was carried out using kinetic model proposed by Mckay et al. which describes the transfer of adsorbate in solution; with the assumption the adsorption obeys the Langmuir model. This model is expressed as follows [16]:

$$\ln\left(\frac{C_t}{C_o} - \frac{1}{1+mK_L}\right) = \ln\frac{mK_L}{1+mK_L} - \frac{1+mK_L}{mK_L}\beta_L S_S t \quad (3)$$

where C_t is the concentration after time t (mg/l), C_o the initial concentration (mg/l), m the mass of adsorbent per unit volume of particle-free adsorbat solution (g/l), K_L the constant obtained by multiplying q^o and b in Langmuir equation (l/g), β_L the mass transfer coefficient (cm/s), and S_S is the outer surface of adsorbent per unit volume of particle free solution (cm^{-1}), given as:

$$S_S = \frac{6m}{D_a d(1-\varepsilon)} \quad (4)$$

where D_a is the particle mean diameter (cm), d the density of adsorbent (g/cm^3) and ε is the porosity of the adsorbent.

As shown in Fig. 3, plot of $\ln(C_t/C_o) - (1/1+mK_L)$ versus t for fluoride gives the straight line. The linear nature of the plot confirms the validity of the diffusion model for the F^-carbon system. The value of mass transfer coefficient β_L was calculated from the slope of the straight-line plot in Fig. 3 and was found to be as 5.2×10^{-6} cm min^{-1} for fluoride. This value indicates that the velocity of F^- transport from liquid phase to the surface of $RS_2/KMnO_4$ carbon is rapid enough to use of this carbon for F^- removal from water. In spite of the transportation of fluoride to solid surface is mainly dependent on agitation and the fluoride concentration in the solution.

3.1.4. Intra-particle diffusion

In the model developed by Weber and Morris, the rate of intra-particle diffusion is a function of $t^{0.5}$ and can be defined by Eq. (5) as follows [17]:

$$q_t = k_p t^{0.5} \quad (5)$$

The intra-particle diffusion rates (k_p) were determined from the plots of q_t versus $t_{0.5}$. If intra-particle diffusion is a rate-controlling step, then the plots should be linear and pass through the origin. In most cases these plots give general features of three stages; initial curved portion, followed by an intermediate linear portion and a plateau. The initial portion due to external mass transfer, the intermediate linear part is due to intra-particle diffusion and the plateau to the equilibrium stage where intra-particle diffusion starts to slow down due to extremely low solute concentrations in the solution.

A plot of the quantity of the anion adsorbed against square-root of time is shown in Fig. 4. It can be observed that the plots are not linear over the whole time range and the graphs of this figure reflect a dual nature, with initial linear portion followed by plateau. This implies that the external surface adsorption (stage 1) is absent and the stage of intra-particle diffusion (stage 2) is attained and continued to 120 min. Finally, equilibrium adsorption (stage 3) starts after 120 min. The anions are slowly transported via intra-particle diffusion into the particles and are finally retained in the pores. Similar dual nature of intra-particle diffusion curve with initial linear portion was found for adsorption of phosphorus onto calcined alunite [18]. The rate constant of intra-particle diffusion was calculated from the slope of the straight line and was found to be 3.05 mg/g $h^{0.5}$ for

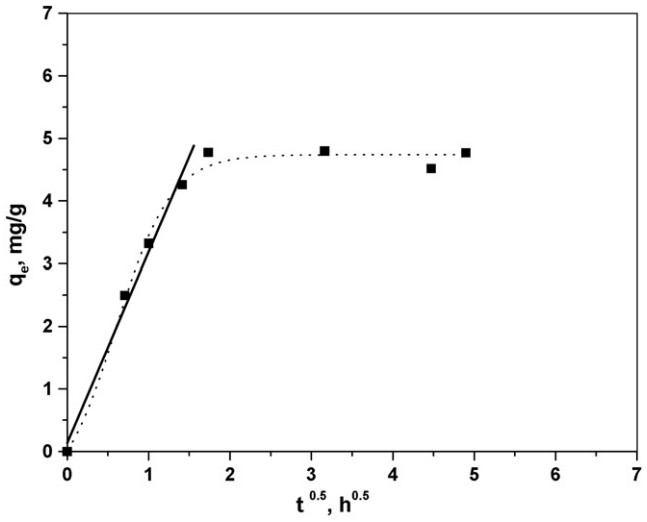

Fig. 4. Intra-particle diffusion plot for F^- adsorption onto $RS_2/KMnO_4$ carbon.

fluoride. However, the linear portion of the curve does not pass the origin and the latter stage of F^- adsorption does not obey Weber–Morris equation. It may be concluded that the adsorption mechanism of this anion from aqueous solution is rather complex process and the intra-particle diffusion was not the only rate-controlling step.

3.2. Effect of concentration

3.2.1. Effect of carbon dose

Fig. 5 shows that increasing the carbon dose increases the percent removal (*R*%) but decreases the adsorption capacity, i.e. increasing the adsorbent dosage increases the percent removal (*R*%) from 20 ml solution containing 20 mg/l of F^- and attained constant removal after a particular carbon dose (optimum dosage) beyond which there is no significant increase in removal. A minimum adsorbent dosage of 30 mg (i.e 1.5 g/l) was required for F^-. There are many factors, which can contribute to this adsorbent dose effect: (i) as the dosage of adsorbent is increased, the adsorption sites remain unsaturated during the

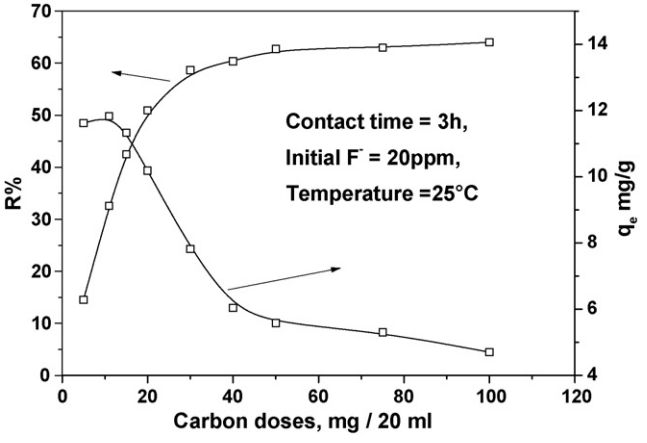

Fig. 5. Effect of carbon doses on adsorption capacity and percent removal of fluoride ion onto $RS_2/KMnO_4$.

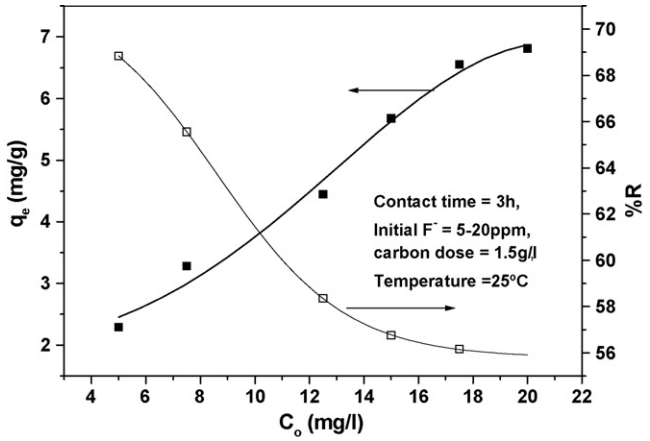

Fig. 6. Influence of fluoride concentration on the percentage adsorption (*R*%) and the equilibrium uptake (q_e) using $RS_2/KMnO_4$ carbon.

adsorption reaction leading to drop in adsorption capacity (q_e) [19]; (ii) the aggregation/agglomeration of sorbent particles at higher doses, which would lead to a decrease in the surface area and an increase in the diffusional path length [20].

3.2.2. Effect of adsorbate concentration

The effect of fluoride concentration on the adsorption process was studied under the optimized conditions of shaking time and carbon dose. Fig. 6 shows that, as fluoride concentration increases, the adsorbed amount of fluoride increases too. However, increase in fluoride concentration beyond about 18 mg/l causes little increase in the amount of fluoride adsorbed indicating that the adsorption sites are almost saturated. Also, the percentage adsorption of F^- decreases with increasing initial concentration of F^-. The percentage is high (>70), but the adsorbed amount is low. This suggests that $RS_2/KMnO_4$ carbon can remove >70% F^- from water if its concentration is below 5 ppm. These results may be explained considering that, at low adsorbate concentration, the ratio of surface active sites to total fluoride is high, hence the fluoride ions could interact with the sorbent to occupy the active sites on the carbon surface sufficiently and be removed from the solution [21]. But with the increase in adsorbate concentration, the number of active adsorption sites is not enough to accommodate fluoride ions.

3.3. Effect of pH

It can be seen that the adsorption of fluoride on $RS_2/KMnO_4$ is strongly pH dependent. Fluoride removal decreases with increasing pH and the removal of fluoride is maximum at pH 2.0. The pH-dependence of fluoride sorption shown in (Fig. 7), is similar to that observed for fluoride adsorption onto aluminum-impregnated activated carbon [22], onto acid treated spent bleaching earth [5], onto low-cost materials [23] $RS_2/KMnO_4$ acquires a positive charge at low pH ($pH < pH_{pzc}$). Therefore, high efficiency in acidic medium can be attributed to the gradual increase in attractive forces and low efficiency in alkaline medium can be explained by the repulsion between the negatively charged surface and fluoride [22,5].

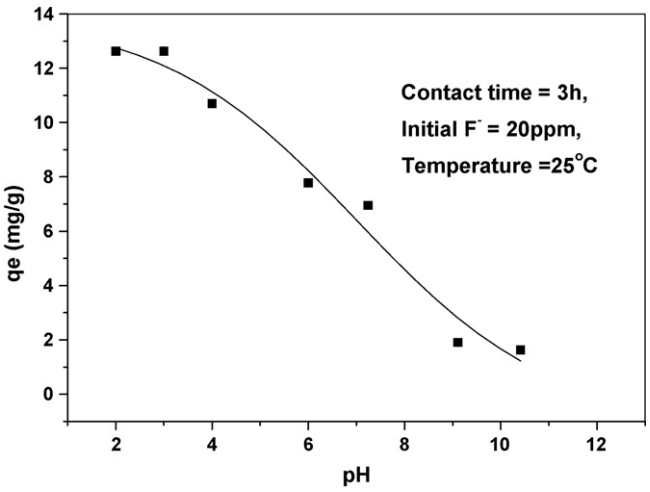

Fig. 7. Effect of pH on the adsorption of F^- by $RS_2/KMnO_4$ carbon.

3.3.1. Possible working mechanisms

The fluoride adsorption can be explained by this two-step ligand exchange reaction mechanism similar to that reported in literature [24,25]:

$$–COH + H^+ \Leftrightarrow –COH_2^+$$

$$–COH_2^+ + F^- \Leftrightarrow –CF + H_2O$$

which give the net reaction

$$–COH + F^- + H^+ \Leftrightarrow –CF + H_2O$$

where –COH represents the surface hydroxyl group.

These reactions indicate that the F^- ion can be considered as fully located on the surface, and the sorption is specific. The pH of the solution after the sorption reaction occurs should increase. In addition, the F^- sorption capacity should increase with decreasing pH [25]. Also, another mechanism can be proposed [25]

$$–COH + F^- \Leftrightarrow –CF + OH^-$$

In that an increase in solution pH there will be competition between the OH^- and F^- ions for the adsorbent site. Eqs. (5) and (4) is valid at very high concentration of fluoride loading per unit weight of $RS_2/KMnO_4$. For both suggested mechanisms, an equivalent number of OH^- must be produced (or H^+ consumed) to maintain electroneutrality [25].

Moreover, the presence of MnO_2 on the carbon surface may participate in the removal of F^- anion.

3.4. Equilibrium adsorption isotherm

The sorption equilibrium isotherm of F^- on $RS_2/KMnO_4$ carbon is given in Fig. 9. According to Giles classification [26], the isotherm was classified as L-type with steep initial portions and a plateau starting at relatively low concentration, the plateau covers a wide range of solution concentrations.

3.4.1. Isotherm modeling

The experimental data of equilibrium isotherm for F^- ions onto $RS_2/KMnO_4$ carbon were modeled using the most frequently used isotherms Freundlich (F), Langmuir (L), and Langmuir–Freundlich (LF) [27]

$$q_e = K_f C_e^{1/n_f} \tag{6}$$

$$q_e = \frac{q^o b C_e}{1 + bC_e} \tag{7}$$

$$q_e = \frac{q^o (bC_e)^{1/n}}{1 + (bC_e)^{1/n}} \tag{8}$$

The isotherm parameters are given in Table 3. The applicability of the isotherm equation is compared by judging the correlation coefficients R^2. In a view of value of R^2, Langmuir and Langmuir–Freundlich isotherm gives satisfactory fit to the experimental data of fluoride.

3.4.2. Dubinin–Radushkevich (D–R) isotherm

To distinguish between physical and chemical adsorption, the adsorption data can be further interpreted by Dubinin–Radushkevich (D–R) isotherm [28]. This isotherm is more general than Langmuir isotherm because it does not assume a homogenous surface or a constant adsorption potential [29].

The D–R equation is given as:

$$q_e = q_m \exp(-B\varepsilon^2) \tag{9}$$

with

$$\varepsilon = RT \ln\left(1 + \frac{1}{C_e}\right) \tag{10}$$

where q_m is the maximum amount adsorbed and can be called the adsorption capacity, B a constant related to the adsorption energy (mol^2/kJ^2), and, ε the potential energy of the surface given by, R the gas constant ($kJ\,mol^{-1}\,K^{-1}$) and T the absolute temperature.The constant B gives the free energy E ($kJ\,mol^{-1}$) of the transfer of 1 mol of solute from infinity to the surface of adsorbent and can be computed using the relationship [30]:

$$E = \frac{1}{\sqrt{2B}} \tag{11}$$

The D–R equation can be linearized as:

$$\ln q_e = \ln q_m - B\varepsilon^2 \tag{12}$$

A plot of $\ln q_e$ versus ε^2 gave straight lines. The values of q_m (mg/g), B (mol^2/kJ^2) and thus the mean free energy of adsorption E ($kJ\,mol^{-1}$) were obtained from the intercept and slope of the straight line.

It is known that the Langmuir and Freundlich isotherm constants do not give any idea about the adsorption mechanism. In order to understand the adsorption type, equilibrium data was tested with Dubinin–Radushkevich isotherm. The plot of $\ln q_e$ against ε^2 for fluoride sorption on $RS_2/KMnO_4$ carbon is shown in Fig. 8. The D–R parameters B and q_m are calculated from the intercept and the slope of the line in Fig. 8, respectively, and the

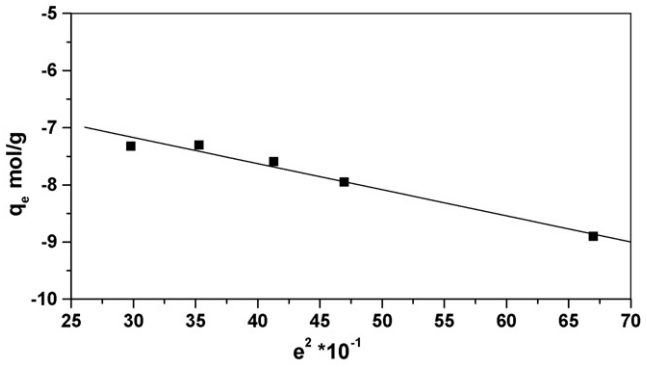

Fig. 8. D–R plot for fluoride sorption onto $RS_2/KMnO_4$ carbon.

Table 2
Values of the D-R parameters for fluoride sorption onto $RS_2/KMnO_4$

	q_m (mg/g)	B (mol^2/kJ^2)	E (kJ mol^{-1})	R^2
Value	57.52	4.57×10^{-3}	10.46	0.97

values are given in Table 2. The mean free energy of adsorption (E), defined as the free energy change when 1 mol of ion is transferred to the surface of the solid from infinity in solution [30] was calculated from b values (Table 2). It is known that magnitude of E is useful for estimating the type of adsorption and if this value is between 8 and 16 kJ mol^{-1}, the adsorption type can be explained by ion exchange [31]. The value of E for F^- ions was found to be ($E = 10.46$ kJ mol^{-1}) and within the energy range of ion exchange. This observation support the ion-exchange mechanism proposed for fluoride adsorption.

3.5. Temperature effect

Fig. 9 shows that temperature has great effect on the adsorption process. As the temperature increased the uptake of F^- onto carbon was decreased. Similar results were reported by Das et al. [32] and by Mohapatra et al. [33].

The isotherm constants that are obtained for the sorption of F^- ions onto $RS_2/KMnO_4$ carbon by the three models:

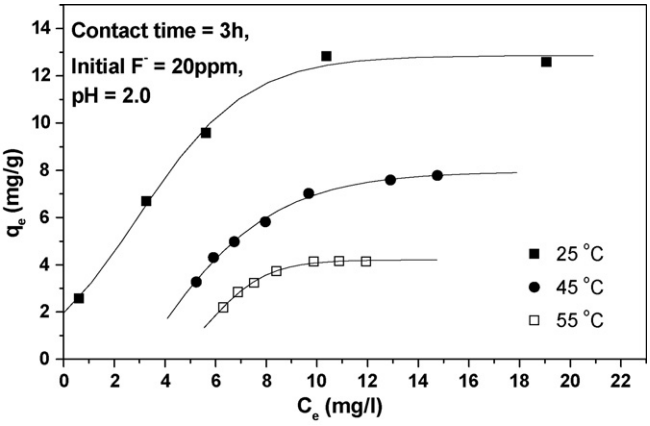

Fig. 9. Temperature effect on fluoride adsorption by $RS_2/KMnO_4$ carbon.

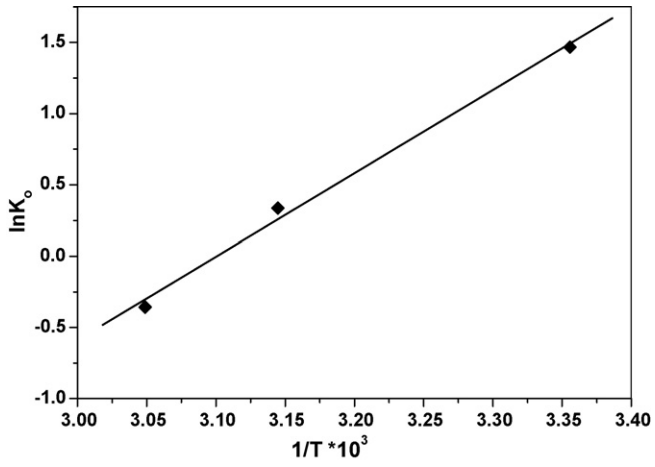

Fig. 10. Van't Hoff plot of F^- sorption onto $RS_2/KMnO_4$ carbon.

Freundlich, Langmuir, and Langmuir–Freundlich at different temperatures are presented in Table 3. Langmuir–Freundlich isotherm presented the experimental data over the whole concentration range with the highest correlation coefficient value, i.e. the Langmuir–Freundlich isotherm provides a good model for this sorption system. The q^o values were found to decrease by increasing temperature. This may be due to raise of temperature affects the solubility of F^- and thus it tends to escape from the solid phase to the bulk phase with increasing temperature of solution.

3.5.1. Thermodynamic parameters

The value of ΔH^o, and ΔS^o were obtained from the slope and intercept of Van't Hoff plot of $\ln K_o$ with the reciprocal temperature $1/T$ as shown in Fig. 10. The thermodynamic equilibrium constant K_o equal to $q^o \times b$ of Langmuir isotherm. The thermodynamic parameters determined for the adsorption of F^- onto $RS_2/KMnO_4$ carbon were determined using the following thermodynamic equations [34]:

$$\ln K_o = \frac{\Delta S^o}{R} - \frac{\Delta H^o}{RT} \quad (13)$$

$$\Delta G^o = -RT \ln K_o \quad (14)$$

where ΔG^o is the standard free energy, R the universal gas constant (1.987 cal/mol K or 8.314 J/mol K) and T is the absolute temperature in Kevin (K). The data are given in Table 4. The exothermic nature of adsorption is indicated by a decrease in K_o with the temperature and the negative value of ΔH^o. The entropy value is negative and suggests no significant change occur in the internal structure of $RS_2/KMnO_4$ carbon during the adsorption [35] and the sorbate ions are stable on the solid surface resulting loss of degrees of freedom at solid/liquid interface [36]. The sorption process causes an increase in the order of the system. The small and negative value of ΔG^o at lower temperature indicates the feasibility of the process and the spontaneous nature of adsorption especially at lower temperature, i.e. the adsorptive forces are strong enough to overcome the potential barrier [37].

It is clear from Table 4 that fluoride sorption is chemical in nature ($\Delta H^o > 10$ kJ mol^{-1}). This may be due to the higher elec-

Table 3
Characteristic parameters of Langmuir, Freundlich and Langmuir–Freundlich models for the adsorption of F^- onto $RS_2/KMnO_4$ carbon

Temperature (°C)	Frundlich			Langmuir			Langmuir–Freundlich			
	K (mg/g)	n	R^2	q^o (mg/g)	b (l/mg)	R^2	q^o (mg/g)	b (1/mg)	n	R^2
25	4.54	2.63	0.90	15.9	0.27	0.97	15.5	0.28	0.95	0.97
45	1.3	1.46	0.9	18.9	0.05	0.92	8.18	0.17	0.3	0.995
55	0.6	1.2	0.83	16.7	0.03	0.84	4.25	0.16	0.15	0.995

Table 4
Thermodynamic parameters of F^- sorption onto $RS_2/KMnO_4$ carbon

Anion	K_o (l/g)			ΔH^o (kJ mol^{-1})	ΔS^o (J/mol K)	ΔG^o (kJ mol^{-1})		
	298 K	318 K	328 K			298 K	318 K	328 K
F^-	4.34	1.4	0.7	−48.6	−150.7	−3.6	−0.9	0.9

tronegativity of fluoride and the specific substitution of fluoride for hydroxide onto $RS_2/KMnO_4$ carbon surface.

3.6. Effect of Co-ions on fluoride adsorption

The influence of coexisting ions, sulphate, chloride and bromide, on fluoride adsorption was studied. Tests were conducted in the presence of 50 ppm of fluoride and 50 ppm each of ion. It was observed that the adsorption capacity for fluoride decreased from 100 to 91% in case of sulphate and to 94% in case of bromide but chloride does not affect fluoride adsorption. It is expected that the presence of anions in solution would enhance coulombic repulsion forces between the anions and fluoride or would compete with fluoride for the active sites [30].

Sulphate had more effect on fluoride adsorption, could be partly attributed to its higher negative charge compared to that of chloride or bromide. Considering the Lewis classification of bases and acids, the order from the weakest to the strongest is: Br^-, Cl^-, F^-, SO_4^{2-} (Bernard and Burnot [38]). Hard acids react preferably and rapidly with soft bases while soft acids similarly react with soft bases [39]. Bromide and chloride are too weak to react with surface functional groups while sulphate relatively strong to compete fluoride but it needs two close surface groups, which reduces its effect.

According to our observation these anions preferred surface sites or mechanisms were different from those of fluoride. It is well documented that fluoride uptake is due to ion exchange and inner-sphere surface complexation, on one hand, while on the other hand, chloride ions form outersphere but sulphate forms partial inner-sphere complexes with sorbents [30]. This high selectivity and affinity for fluoride adsorption, makes $RS_2/KMnO_4$ carbon a highly suitable sorbent for water treatment applications.

3.7. Effect of NOM on fluoride adsorption

The effect of natural organic matter on the adsorption of F^- onto $RS_2/KMnO_4$ was discussed using the surface water of Ismailia canal. Fig. 11 shows the isotherm tests of fluoride

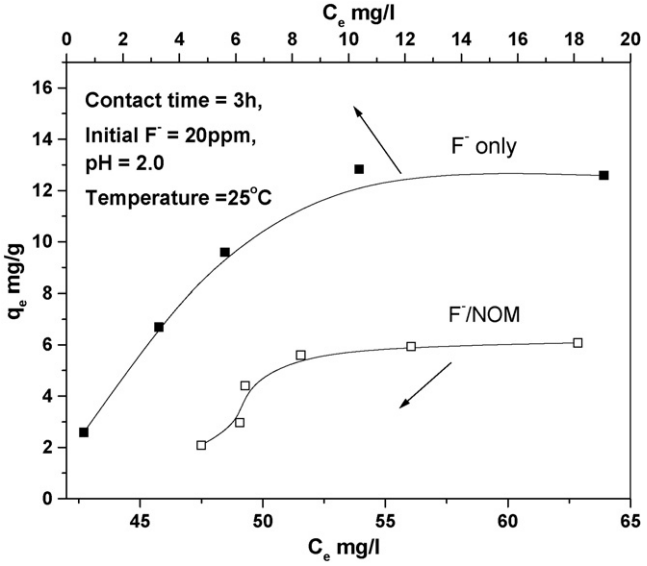

Fig. 11. Effect of NOM on fluoride adsorption.

adsorption onto $RS_2/KMnO_4$ carbon using natural water compared to bidistilled water. The Langmuir–Frundlich constants were listed in Table 5. As can be seen, the presence of the NOM decreases F^- adsorption. NOM has negative charged molecules (attributed to carboxylic acid and phenolic functionalities) [40] can compete with fluoride for the available active sites on carbon surface. The process reduction of carbon adsorption capacity due to presence of NOM is known as "carbon fouling" and is of particular concern in water treatment plants [40].

Table 5
Langmuir-Frundlich constants of F^-:($RS_2/KMnO_4$) adsorption system (with/without) NOM

Parameter	F^-	F^-/NOM
q^o (mg/g)	15.5	5.7
b	0.28	0.021
n	0.95	0.03
R^2	0.97	0.94

Table 6
Comparison of fluoride sorption capacity using $RS_2/KMnO_4$ carbon with published data

Adsorbent	q^o (mg/g)	Reference
$RS_2/KMnO_4$	15.9	This work
Acid treated spent bleaching earth	7.75	[5]
Lignite	7.1	[42]
Bituminous coal	7.44	[43]
Fly ash	20	[5]
Hydroxyapatite	4.54	[15]
Fluorspar	1.79	[15]
Calcite	0.39	[15]
Quartz	0.19	[15]
AlC-300 carbon	1.07	[22]
Plain activated carbon	0.49	[22]
La^{3+}-impregnated cross-linked gelatin	21.3	[44]
Activated alumina	2.41	[45]
China clay	0.66	[37]
Zn/Al hydrotalcite	16.2	[32]
Activated red mud	6.3	[3]
Original red mud	3.11	[3]
α-Alumina	8.42	[46]
γ-Alumina	12.04	[47]
Polymeric resin IRA-410	18.88	[46]

3.8. Comparison with other adsorbents

The adsorptive capacity of $RS_2/KMnO_4$ to remove fluoride has been compared with those of other adsorbents reported in the literature (Table 6). Although, these values were obtained at different pH range they can be useful criterion of the adsorbent capacity. It can be seen that $RS_2/KMnO_4$ carbon exhibits considerably greater F^- adsorption potential when compared by less-attractive and low-cost materials. It is important to emphasize that the specific surface area of aluminum-impregnated activated carbon at 300 °C (ALC-300) and plain carbon are 950 and 1044 m^2/g, respectively [22], which are higher than that of $RS_2/KMnO_4$, but their fluoride adsorption capacity is much lower than that of $RS_2/KMnO_4$. This is due to unique structure of $RS_2/KMnO_4$. Also, $RS_2/KMnO_4$ have q^o value comparable with polymeric resin IRA-410 and fly ash. This result is very interesting since fly ash has a very small surface area. It is known that fly ash contains SiO_2 and Al_2O_3 as the major constituents and be responsible for the adsorption [5]. However, based on the adsorbent mass, the comparison between these adsorbents was necessary to decide the required mass to reduce the F^- concentration from 4 ppm (average of F^- concentration in potable water) to 1 ppm (reasonable concentration for health standard). In this concern, the amount of adsorbent was estimated using a mass balance equation [22,41].

$$VC_o = mq + VC_f \quad (15)$$

Because q and C_f must be in equilibrium, q for $RS_2/KMnO_4$ can be calculated by substituting $q^o = 15.9$ and $b = 0.27$ of Langmuir equation, C_o, C_f and V are 4, 1 mg/l and 1 m^3, respectively. The results are listed in Table 7.

Activated rice straw carbon treated by $KMnO_4$ exhibits promising results. The mass required for $RS_2/KMnO_4$ is only 0.9 kg, which is greatly less than plain carbon (40.5 kg), 6.0, 4 and 1.5 times less than that of the AlC-300 carbon (5.6 kg), α-alumina (3.6 kg) and γ-Al_2O_3 (1.3 kg), respectively, and is greater to that of IRA-410 polymeric resin (0.3 kg) and Al_2O_3 supported on carbon nanotubes, Al_2O_3/CNTs (0.31 kg) [41]. These results indicate that $KMnO_4$ modified activated carbon produced from rice straw has a large potential to be an adsorbent for fluoride removal. The high adsorption capacity for this material is probably related to the sorption mechanism including both ion exchange and complexation.

Table 7
Mass of adsorbent required to decrease the fluoride concentration from 4 to 1 mg/l in solution volume 1 m^3

Adsorbent	q (mg/g)	V/m (l/g)	m (kg)
$RS_2/KMnO_4$	3.4	1.13	0.9
Plain carbon	0.07	0.025	40.5
Al_2O_3/CNTs	9.68	3.2	0.31
AlC-300 carbon	0.54	0.179	5.6
α-Alumina	0.82	0.273	3.6
γ-Alumina	2.25	0.75	1.3
IRA-410 polymeric resin	10.0	3.33	0.3

3.9. Application: fluoride removal from phosphoric acid

The presence of fluorine in the phosphoric acid is undesirable. This may cause corrosion or precipitation problems in the evaporators during the concentration of the acid. It will also contaminate the fertilizer produced from such acid and therefore will lower its P_2O_5 content [48].

The ability of $RS_2/KMnO_4$ carbon to remove F^- from Egyptian crude phosphoric acid ($P_2O_5 = 48.42\%$) was tested. Isotherm experiments were carried out by mixing 10 ml of crude phosphoric acid with various masses of $RS_2/KMnO_4$ carbon ranged (0.1–1.0 g) at 25 °C. The adsorption isotherm of fluoride from phosphoric acid was presented in Fig. 12 and the Langmuir–Frundlich parameters were calculated and listed in Table 8. It clear that the adsorptive capacity, q^o, of fluoride in phosphoric acid is greater than in distilled water. This may be

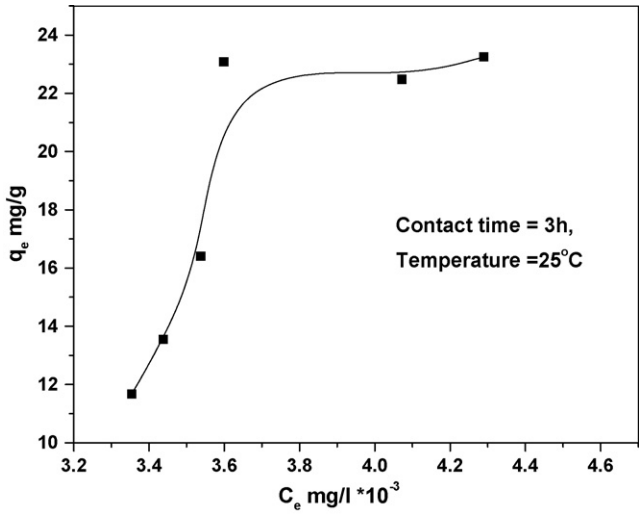

Fig. 12. Adsorption isotherm of fluoride in phosphoric acid.

Table 8
Langmuir-Frundlich parameters of fluoride adsorption onto $RS_2/KMNO_4$ in distilled water and phosphoric acid

Parameter	Distilled water	Phosphoric acid
q^o (mg/g)	15.5	23.3
b (l/g)	0.28	2.96
n	0.95	0.035

due to the pH in phosphoric reach zero which highly enhance fluoride adsorption onto $RS_2/KMnO_4$.

4. Conclusion

On the basis of this study it is concluded that $KMnO_4$-modified activated carbon derived from steam pyrolysis of rice straw has good potential as a cheap and effective scavenger for fluoride anion present in aqueous solutions and can be effectively utilized for waste management and environmental protection purposes. The factors influencing adsorption process of F^- by this carbon showed that reaction rate was fast and temperature dependent.

The main conclusions that can be drawn from batch adsorption study are given below:

(1) The solution pH was the most important parameter affecting adsorption. The optimum pH for maximum adsorption was determined to be 2.0 for fluoride.
(2) The adsorption followed Langmuir–Freundlich isotherm.
(3) Fluoride sorption is better occurred at lower temperature.
(4) The presence of NOM decreases F^- adsorption.

The results obtained in this study are expected to provide useful guidelines for engineers and chemists who work in waste water systems.

References

[1] N.N. Greenwood, A. Earnshaw, Chemistry of the Elements, Pergamon Press, Toronto, 1984.
[2] G. de la Puente, J.J. Pis, J.A. Menhdez, P. Grange, Thermal stability of oxygenated functions in activated carbons, J. Anal. Appl. Pyrolysis 43 (1997) 125–138.
[3] Y. Cengeloğlu, E. Kir, M. Ersöz, Removal of fluoride from aqueous solution by using red mud, Sep. Purif. Technol. 28 (2002) 81–86.
[4] R. Helmer, Water quality and health, Environmentalist 19 (1999) 11.
[5] M. Mahramanlioglu, I. Kizilcikli, I.O. Bicer, Adsorption of fluoride from aqueous solution by acid treated spent bleaching earth, J. Fluorine Chem. 115 (2002) 41–47.
[6] A.A.M. Daifullah, Removal of ^{226}Ra, Fe^{3+} and Mn^{2+} from ground water using modified activated carbon, Isotope Radiat. Res. 35 (1) (2003) 77–93.
[7] A.N.A. El-Hendawy, Influence of HNO_3 oxidation on the structure and adsorptive properties of corncob-based activated carbon, Carbon 41 (2003) 713–722.
[8] G. Mckay, Use of Adsorbent for the Removal of Pollutants from Wastewater, CRC press, NY, 1996.
[9] Y. Leon, C.A. Leon, J.M. Solar, V. Calemma, L.R. Radovic, Evidence for the protonation of basal plane sites on carbon, Carbon 30 (1992) 797–811.
[10] T.J. Bandosz, J. Jagiello, J.A. Schwarz, Comparison of methods to assess surface acidic groups on activated carbon, Am. Chem. Soc. 64 (1992) 891–895.
[11] Y.-H. Li, S. Wang, X. Zhang, J. Wei, C. Xu, Z. Luan, D. Wn, Adsorption of fluoride from water by aligned carbon nanotubes, Mater. Res. Bull. 38 (2003) 469–476.
[12] Y.S. Ho, G. McKay, Pseudo-second order model for sorption processes, Process Biochem. 34 (1999) 451–465.
[13] A. Gücek, S. Sener, S. Bilgen, M.A. Mazmanc, Adsorption and kinetic studies of cationic and anionic dyes on pyrophyllite from aqueous solutions, J. Colloid Interface Sci. 286 (2005) 53–60.
[14] L. Ruixia, G. Jinlong, T. Hongxiao, Adsorption of fluoride, phosphate, and arsenate ions on a new type of ion exchange fiber, J. Colloid Interface Sci. 248 (2002) 268–274.
[15] X. Fan, D.J. Parker, M.D. Smith, Adsorption kinetics of fluoride on low cost materials, Water Res. 37 (2003) 4929–4937.
[16] H. Tran, F.A. Roddick, Comparison of chromatography and desiccant silica gel for the adsorption of metal ions. I: Adsorption and kinetics, Water Res. 33 (1999) 2992–3000.
[17] W.J. Weber, J.C. Morris, Kinetics of adsorption on carbon from solutions, J. Sanit. Eng. Div. Am. Soc. Civ. Eng. 89 (SA2) (1963) 31.
[18] M. Özacar, Equilibrium and kinetic modelling of adsorption of phosphorus on calcined alunite, Adsorption 9 (2003) 125–132.
[19] D.C. Sharma, C.F. Forster, Removal of hexavalent chromium using sphagnum moss peat, Water Res. 27 (1993) 1201–1208.
[20] M. Özacar, I.A. Sengil, Adsorption of metal complex dyes from aqueous solutions by pine sawdust, Bioresour. Technol. 96 (2005) 791–795.
[21] S.F. Montanher, E.A. Oliveira, M.C. Rollemberg, Removal of metal ions from aqueous solutions by sorption onto rice bran, J. Hazard. Mater. B117 (2005) 207–211.
[22] R.L. Ramos, J. Ovalle-Turrubiartes, M.A. Sanchez-Castillo, Adsorption of fluoride from aqueous solution on aluminum-impregnated carbon, Carbon 37 (1999) 609–617.
[23] M. Srimurali, A. Pragathi, J. Karthikeyan, A study on removal of fluorides from drinking water by adsorption onto low-cost materials, Environ. Pollut. 99 (1998) 285–289.
[24] A.M. Raichur, M.J. Basu, Adsorption of fluoride onto mixed rare earth oxides, Sep. Purif. Technol. 24 (2001) 121–127.
[25] Y. Wang, E.J. Reardon, Activation and regeneration of a soil sorbent for defluoridation of drinking water, Appl. Geochem. 16 (2001) 531–539.
[26] C.H. Giles, T.H. MacEwan, S.N. Nakhawa, A. Smith, Studies in adsorption Part XI A system of classification of solution adsorption mechanism and in measurement of specific surface areas of solids, J. Chem. Soc. 111 (1960) 2993–3973.
[27] S. Al-Asheh, F. Banat, R. Al-Omari, Z. Duvnjak, Predictions of binary sorption isotherms for the sorption of heavy metals by pine bark using single isotherm data, Chemosphere 41 (2000) 659–665.
[28] M.M. Dubinin, L.V. RadushKevich, The equation of the characteristic curve of the activated charcoal, Proc. Acad. Sci. U.S.S.R., Phys. Chem. Sect. 55 (1947) 331.
[29] A. Kilislioglu, B. Bilgin, Thermodynamic and kinetic investigations of uranium adsorption on amberlite IR-118H resin, Appl. Radiat. Isotopes 58 (2003) 155–160.
[30] M.S. Onyango, Y. Kojima, O. Aoyi, E.C. Bernardo, H. Matsuda, Adsorption equilibrium modeling and solution chemistry dependence of fluoride removal from water by trivalent-cation-exchanged zeolite F-9, J. Colloid Interface Sci. 279 (2004) 341–350.
[31] F. Helferrich, Ion Exchange, McGraw-Hill, New York, 1962, p. 162.
[32] D. Das, J. Das, K. Parida, Physicochemical characterization and adsorption behavior of calcined Zn/Al hydrotalcite-like compound (HTlc) towards removal of fluoride from aqueous solution, J. Colloid Interface Sci. 261 (2003) 213–220.
[33] D. Mohapatra, D. Mishra, S.P. Mishra, G. Roy Chaudhury, R.P. Das, Use of oxide minerals to abate fluoride from water, J. Colloid Interface Sci. 275 (2004) 355–359.
[34] M. Sekar, V. Sakthi, S. Rengaraj, Kinetics and equilibrium adsorption study of lead(II) onto activated carbon prepared from coconut shell, J. Colloid Interface Sci. 279 (2004) 307–313.
[35] V.K. Gupta, A. Mittal, V. Gajbe, Adsorption and desorption studies of a water soluble dye, Quinoline Yellow, using waste materials, J. Colloid Interface Sci. 284 (2005) 89–98.

[36] C. Raji And, T.S. Anirudhan, Batch Cr(VI) removal by polyacrylamide-grafted sawdust: kinetics and thermodynamics, Water Res. 32 (1998) 3772–3780.
[37] A.K. Chaturvedi, K.C. Pathak, V.N. Singh, Fluoride removal from water by adsorption on China clay, Appl. Clay Sci. 3 (1988) 337–346.
[38] M. Bernard, F. Burnot, Usuel de Chimie Générale et Minérale, Dunod, Paris, 1996, p. 562.
[39] K. Jaafari, S. Elmaleh, J. Coma, K. Benkhouja, Equilibrium and kinetics of nitrate removal by protonated cross-linked chitosan, Water SA 27 (2001) 9–14.
[40] M. Bjelopavlic, G. Newcombe, R. Hayes, Adsorption of NOM onto activated carbon: effect of surface charge, ionic strength, and pore volume distribution, J. Colloid Interface Sci. 210 (1999) 271–280.
[41] Y.-H. Li, S. Wang, A. Cao, D. Zhao, X. Zhang, C. Xu, Z. Luan, D. Ruan, J. Liang, D. Wu, B. Wei, Adsorption of uoride from water by amorphous alumina supported on carbon nanotubes, Chem. Phys. Lett. 350 (2001) 412–416.
[42] A. Sivasayamy, P. Singhkunwar, D. Mohan, M. Maruthamuthu, Studies on defluoridation of water by coal-based sorbents, J. Chem. Technol. Biotechnol. 76 (2001) 717–722.
[43] A.K. Chaturvedi, K.P. Yadava, K.C. Pathak, V.N. Singh, Defluoridation of water by adsorption on fly ash, Water Air Soil Pollut. 49 (1990) 51–61.
[44] Y. Zhou, C. Yu, Y. Shan, Adsorption of fluoride from aqueous solution on La^{3+}-impregnated cross-linked gelatin, Sep. Purif. Technol. 36 (2004) 89–94.
[45] Ghorai, K.K. Pant, Equilibrium, kinetics and breakthrough studies for adsorption of fluoride on activated alumina, Sep. Purif. Technol. 42 (2005) 265–271.
[46] T.J. Ovall, M.Sc. Thesis in chemical engineering Faculted de Ciencias Quimicas, Unversidad Auto'noma de San luis Potosi, Mexico, 1996.
[47] Y.C. Wu, A.J. Nilya, Environ. Eng. Div. 105 (EE2) (1979) 357.
[48] Z. Qafas, K. El Kacemi, E. Ennaassia, M.C. Edelahi, Study of the removal of fluoride from phosphoric acid solutions by precipitation of Na_2SiF_6 with Na_2CO_3, Sci. Lett. 3 (2002) 1–5.